Available free online at www.medjchem.com

Mediterranean Journal of Chemistry 2011, 1(2), 44-55

Telon dye removal from Cu(II)-containing aqueous media using p-diphosphonium organo-montmorillonite

Benamar Makhoukhi[1], Mohamed Amine Didi[1*], Hidayet Moulessehoul[1], Abdelkrim Azzouz[2*]

[1]Laboratory of Separation and Purification Technology, Department of Chemistry, Tlemcen University, Box 119, Tlemcen, Algeria

[2]University of Quebec at Montreal, Department of Chemistry, Canada H3C3P8

Abstract: Ion-exchange of montmorillonite with para-bis(triphenyl phosphonium methylene)-benzene ions (p-TPhPMB) provided an organo-montmorillonite adsorbent with improved affinity towards Telon dyes. Adsorption tests applied to Telon-red and Telon-blue in the presence of Cu(II) cations revealed a significant increase in the maximum adsorption capacity from ca. 11-26 for the starting clay mineral to ca. 110-160 $mg.g^{-1}$ after intercalation. This improvement was attributed to increases in both the organophilic character towards the organic dyestuffs investigated and the interlayers spacing. Besides dye-diphosphonium and Cu(II)-diphosphonium interactions, dye adsorption on organo-montmorillonite also involved the formation of Cu(II) exchanged Telon-dye species. It was found that dye adsorption involves not only binary interactions between the three chemical species, but also synergy due to a possible bridging action of the divalent Cu(II) cations. On organo-Mt, the organophilic character was a key factor for higher amounts of adsorbed dye.

Key words: organo-montmorillonite, diphosphonium salts, adsorption, Telon-dyes, copper.

Introduction

Treatments of wastewaters containing hazardous pollutants like organic dyes still remains a major issue, because of the cause negative impacts upon environment, biodiversity and even human health. Dye retention on natural materials, more particularly on clay-based adsorbents, may be a convenient route. In this regard, montmorillonite-rich materials like bentonites have shown promising prospects[1-7]. Montmorillonite, the main component of bentonites, displays interesting surface properties that can be thoroughly tailored for such a purpose via intercalation with chemical species[8,9]. For instance, insertion of organic cations within the interlayer space ought to enhance the organophilic interactions, inducing thereby improved affinity towards organic compounds[10-16].

Diphosphonium ion-exchanged montmorillonite already turned out to be quite effective in removing polluting dyestuffs[10,17-19]. Moreover, the presence of metal cations is expected to induce mordanting phenomena that enhance the interactions occurring between the dye molecules and absorbent. In other words, metal cations will act as a mordant[20], via combination with the dyestuff particles into coordination compounds that are strongly adsorbed by certain solid surfaces.

Mordanting techniques commonly use metal cations (Al^{3+}, Cr^{3+}, Co^{2+}, Ni^{2+}, Cu^{2+}, Fe^{2+}, etc) to retain or reinforce stains for dyeing fabrics in textile industries or in tissue and cell preparation in biology and biochemistry[21,22].

**Corresponding authors:*
madidi13@yahoo.fr; abdelkrimazzouz@uqam.ca; Tel:+213552639237

Insertion of Cu(II) cations within the interlayer space of montmorillonite promotes interactions with phenanthroline and the formation of $Cu(Phen)_3$–bentonite complex[23]. This resulted in an increase in the d_{001} basal spacing from 14.24 to 17.7 Å. Other works[24] have shown that heavy metals like palladium and cadmium and organic pollutants can be simultaneously and efficiently retained on bentonite, without competitive adsorption. Pd(II)-organic complexes have also been immobilized on Na-montmorillonite via ion-exchange[25].

Immobilization of metal complexes on montmorillonite has already found application in heterogeneous catalysis[26].

So far, various adsorbents such as clays, coals and others have been used to immobilize organic pollutants[27,28]. Among clay minerals, bentonite, and more particularly its main constituent, montmorillonite is focusing a growing interest, due to its cation exchange capacity, high adsorption capacity, which can be modulated by increasing the specific surface and its affinity for organic and inorganic ions. For metal cations, montmorillonite is regarded as being the most suitable adsorbent, acting by ion exchange[29].

In continuation of a previous study on Telon-dye removal by diphosphonium exchanged montmorillonites[10], the performances of the most effective of these organo-Mts, namely the p-organo-Mt, in the removal of the same dyestuffs in the presence of Cu (II) ions are reported herein. In the present investigations, montmorillonite was ion-exchanged with para-diphosphonium ions, and attempts were performed to retain Telon-red and Telon-blue dyes in the presence of Cu(II) ions. The interactions involved in the adsorption process were examined though kinetics and equilibrium studies.

Results and Discussion

Telon-dye-Cu(II) interaction

Figure 1 shows the spectra of Telon-red and Telon-blue in the absence of Cu(II) ion. Prior to adsorption attempts, various Telon-Cu(II) solutions were obtained by mixing a constant Cu(II) amount (0.01 M) with various dye quantities (10 - 400 $mg.L^{-1}$), and conversely by mixing a constant dye amount (400 $mg.L^{-1}$) with various Cu(II) quantities. For both Telon dyes, no wavelength shifts were observed and no new absorbance appeared. This suggests that under these conditions, Cu(II)-Telon-dye combination should proceed mainly via ion exchange, and that chelation with both dyestuffs, if any, must not contribute significantly (Figures 2 and 3).

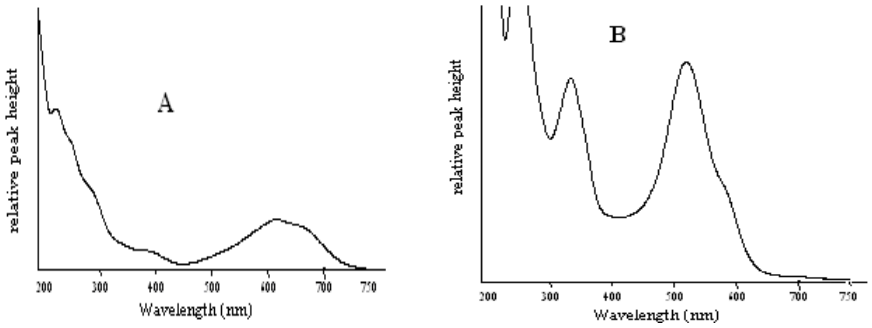

Figure 1. UV-Vis absorbance of Telon-blue (A) and Telon-red (B)

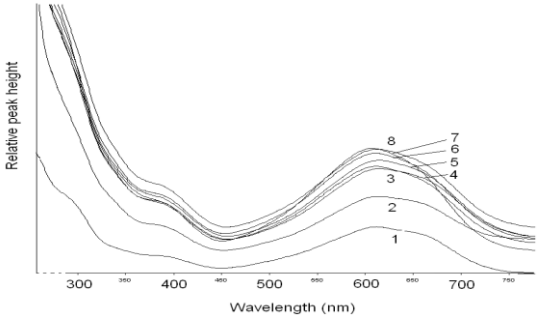

Figure 2. UV-Vis absorbance of Telon-blue (400 mg.L^{-1}) at various Cu(II) concentrations:

1. 0.002; 2. 0.003; 3. 0.004; 4. 0.006; 5. 0.007; 6. 0.008; 7. 0.009 mg.L^{-1}.

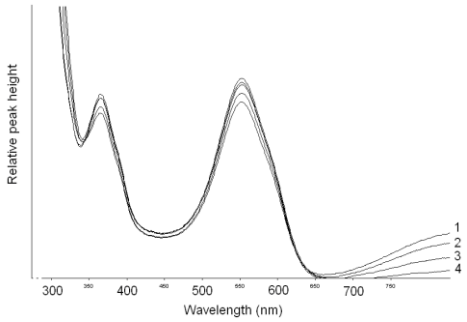

Figure 3. UV-Vis absorbance of Telon-red (400 mg.L^{-1}) at various Cu(II) concentrations:

1. 0.002; 2. 0.004; 3. 0.006; 4. 0.008 mg.L^{-1}.

Therefore, one must expect that the adsorption process will involve Cu(II) exchanged Telon dye molecules, and that both dispersed and exchanged Cu(II) cations will act as bridging species between the anionic Telon-dye organic moieties and clay mineral surface, more particularly on NaMt[1,30,31]. On organo-Mt, organophilic interactions between Telon-dye molecules and the p-diphosphonium moiety should be predominant.

Dye-Cu(II adsorption on NaMt

As a general feature, in the presence of Cu^{2+} ions, Qt increased in time for both Telon-red and Telon-blue dyes (Figure 4). Interestingly, both $\boldsymbol{Q_{max}}$ values were higher than those obtained in Cu-free aqueous media by a factor of ca. 6.25 and 3.5, respectively[10]. This provided clear evidence that the mere presence of Cu^{2+} ions enhanced significantly dye adsorption. Nonetheless, these values accounted for ca. 0.16 (Telon-red-Cu) and 0.07 mmol. g^{-1} (Telon-blue-Cu), which still remain much lower than the CEC value of NaMt (0.95 meq. g^{-1}). Here also the contribution of cation exchange sites to telon dyes adsorption, if any, might not be significant.

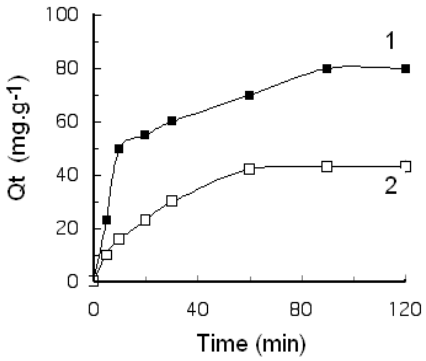

Figure 4. Evolution in time of the amount of adsorbed Telon dye on NaMt.
1**.** Telon-red; 2**.** Telon-blue.
T = 21°C; [Telon-dye] = 100 mg/L; [Cu(II)] = 0.01 M.

Equilibrium was attained after ca. 90 and 60 min, respectively, and the maximum amount of adsorbed Telon-red ($\boldsymbol{Q_{max}}$= 80 mg.g^{-1}) was ca. twice higher than that of Telon-blue (42 mg. g^{-1}). Here, one must expect that adequate kinetic models will provide respective rate constants in the same ratio.

Adsorption kinetics on NaMt

Kinetic study attempts using both the pseudo-first and pseudo-second order models[32-34] were achieved by plotting respectively, versus time (t):

$$Log[Q_{\max} - Q_t] = LogQ_{\max} - (k_1 / 2{,}303).t \qquad (1)$$

$$\frac{t}{Q_t} = \frac{t}{Q_{\max}} + \frac{1}{k_2.Q_{\max}^2} \qquad (2)$$

where k_1 and k_2 were the global rate constants of 1st Order and 2nd Order respectively.
No linearity was obtained for the pseudo-first order model within the whole investigated time gap (Figure 5), but highly linear evolution of ***t/Qt*** in time was noticed when the pseudo-second order model was applied (Figure 5).

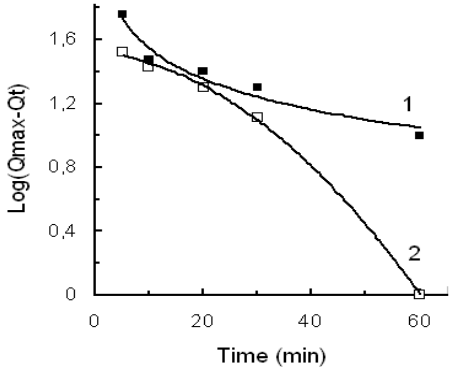

Figure 5. Pseudo-first order model for Telon-dye adsorption on NaMt.
1**.** Telon-red; 2**.** Telon-blue.
T = 21°C; [Telon-dye] = 100 mg/L; [Cu(II)] = 0.01 M.

However, deeper analysis of the first order plot (Figure 5) revealed certain linearity within the first 30 min gap for both Telon-dyes, but as the process evolved in time, a loss of linearity was observed. Calculation attempts according to the pseudo-first order model[35] gave

inaccurate values of the rate constant with estimated correlation coefficients (R^2) of 0.91 for Telon-red-Cu and 0.93 for Telon-blue-Cu (Table 1).

Table 1. Calculations of the global rate constants

Telon dye	Pseudo order models				Diffusion model			
	1st Order	2nd Order						
	R^2	Q_{max}(mg.g^{-1})	k_2 (min.g^{-1}.mg^{-1})	R^2	K_d (mg.g^{-1}.min$^{-0.5}$)		R^2	
Red	0.91	91 ± 5	1.23 .10^{-3}	0.98	15.81[a]	4.36[b]	0.94[a]	0.98[b]
Blue	0.93	51 ± 5	5.94 .10^{-4}	0.97	5.42		0.96	

K_d is the kinetic coefficient: a Estimated for the first diffusion step (external diffusion);

b Estimated for the second diffusion step (intra-particle diffusion).

Therefore, pseudo-first order kinetics might govern the initial step of dye adsorption, but cannot be applied throughout the entire process, because the dye concentration and pH also evolve over time, inducing unavoidable change in the mechanisms pathway, as already reported[10].

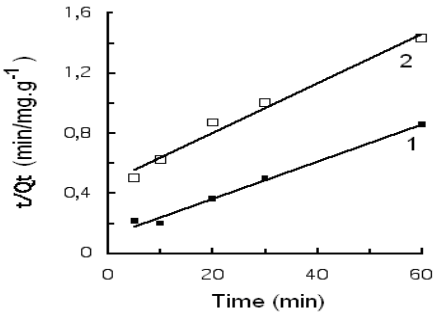

Figure 6. Pseudo-second order for Telon-dye adsorption on NaMt.

1**.** Telon-red; 2**.** Telon-blue.

T = 21°C; [Telon-dye] = 100 mg/L; [Cu(II)] = 0.01 M.

R^2 values closer to unity of 0.98 for Telon-red and 0.97 for Telon-blue indicated that the adsorption of both dyes on NaMt obeyed better the pseudo-second order model, as well supported by the highly linear increase of t/Qt in time (Figure 6). As expected, the rate constant k_1 (1.23.10^{-3}) was ca. twice higher than k_2 (5.94.10^{-4}), indicating that Telon-red adsorbed on NaMt twice faster than Telon-blue.

Interparticle and intraparticle diffusion on NaMt

Seemingly, diffusion phenomena played key-roles in process limitation but only for Telon-blue, because when applying the intra-particle diffusion model[36], linear proportionality occurred between ***Qt*** and $t^{0.5}$ (Figure 7). The diffusion rate constant (K_d), defined as being the straight line slope, was found to be equal to 5.42 mg.g^{-1}.min$^{-0.5}$ with a correlation coefficient (R^2) close to unity. This provided clear evidence that a single pathway was involved in the mechanisms of Telon-blue adsorption, and did not change over time. This suggests that Telon-blue molecules did not accumulate at the pore entry, presumably due to the nearly linear shape of Telon-blue molecules as compared to Telon-red.

Deeper insights in the curve shape for Telon-red showed two linear portions around $t^{0.5}$ = 3, corresponding to the occurrence of at least two consecutive steps, most likely external and internal diffusion. The slopes of both curve portions gave diffusion rate constants of 15.81 (K_{d1}) and 4.36 mg.g^{-1}.min$^{-0.5}$ (K_{d2}) with R^2 values close to unity. The ratio between these

values is of ca. 3.5, and suggested the occurrence of a relatively fast external diffusion, followed by an internal diffusion ca. three times slower. As a consequence, Telon-red-Cu must accumulate at the pore entry, and a much slower intraparticle or pore diffusion must take place, most likely due to its relatively bulkier molecular configuration and higher critical molecular size.

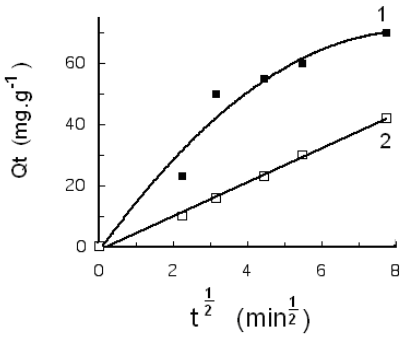

Figure 7. Qt versus $t^{0.5}$ for Telon-dye adsorption on NaMt.
1**.** Telon-red; 2**.** Telon-blue.
T = 21°C; [Telon-dye] = 100 mg/L; [Cu(II)] = 0.01 M.

Interestingly, K_d was ca. three times smaller than K_{d1}, indicating that for Telon-red the mass transfer towards the external surface occurred three times faster than for Telon-blue. Thus, it clearly appears that for Telon-red, the intra-particle diffusion turned out to be a rate-limiting step, but not throughout the entire duration of the adsorption process.

Adsorption isotherms on NaMt

Deeper insights in the adsorption process were achieved through isotherm investigations. A first overview to figures 8 and 9 suggested that dye adsorption did not fit Langmuir's model, because no linearity was noticed for both Telon-red and Telon-blue dyes.
The Langmuir isotherm is represented by:

$$\frac{C_e}{Q_e} = \frac{1}{Q_0 b} + \frac{C_e}{Q_0} \qquad (3)$$

where Ce is the equilibrium concentration ($mg.L^{-1}$), Q_e the amount adsorbed at equilibrium and Q_0 and b are Langmuir constants related to adsorption capacity and energy of adsorption, respectively.

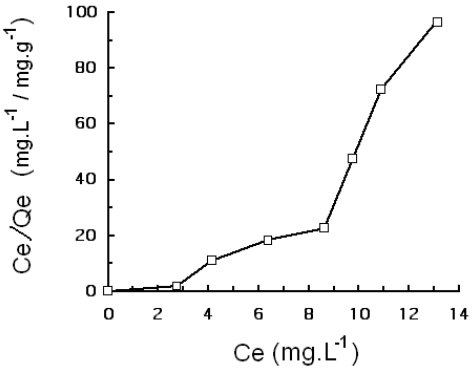

Figure 8. Langmuir adsorption isotherm for Telon-blue on NaMt.
T = 21°C; [Telon-dye] = 100 mg/L; [Cu(II)] = 0.01 M.

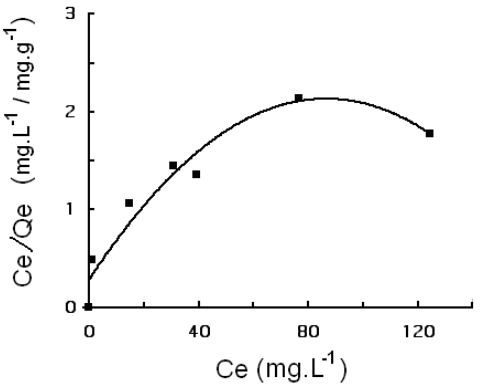

Figure 9. Langmuir adsorption isotherm for Telon red on NaMt.
T = 21°C; [Telon-dye] = 100 mg/L;
[Cu(II)] = 0.01 M.

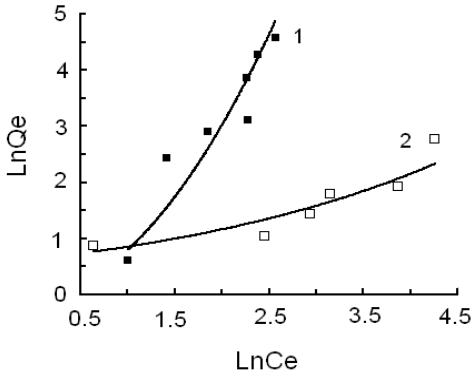

Figure 10. Freundlich adsorption isotherms on NaMt.
1**.** Telon-red; 2**.** Telon-blue.
T = 21°C; [Telon-dye] = 100 mg/L;
[Cu(II)] = 0.01 M.

The Freundlich isotherm is represented by:

$$Q_e = K.C_e^n \qquad (4)$$

where Ce is the equilibrium concentration ($mg.L^{-1}$), K and n are the Freundlich parameters.

In contrast, Freundlich's model turned out to be more adequate to describe both Telon-dye adsorption on NaMt within the investigated concentration ranges, inasmuch as almost linear isotherms were obtained (Figure 10). Telon-red adsorption better obeyed Freundlich's model with an $\boldsymbol{R^2}$ value for Telon-red-Cu (**0.97**) slightly higher than for Telon-blue **(0.95)** (Table 2). In addition, the slightly higher adsorption constant for Telon-red (**0.33**) as compared to Telon-blue-Cu (**0.26**) confirmed once again the stronger affinity of Telon-Red for the surface of NaMt.

Table 2. Freundlich constant for adsorption on NaMt.

Telon-dye	K	N	R^2
Blue	0.26	2.24	0.95
Red	0.333	1.404	0.97

Effect of dye concentration

Before and after intercalation with p-diphosphonium cations, dye concentration (***Ce***) had significant effects on the amount of adsorbed dye, inasmuch as an increase of this factor induced an increase of ***Qe*** (Figures 11 and 12).

The amount of dye or copper fixed per gram of adsorbent at equilibrium was determined by the following relation (5):

$$Q_e = (C_0 - C_e).V / m \qquad (5)$$

where C_0 and C_e denote the initial and at equilibrium concentrations of dye in the aqueous phase (mg/g), V is the volume of the aqueous phase (L), m is the weight of adsorbent used (g).

For both Telon-red and Telon-blue, an almost linear dependence occurred below a dye concentration level of ca. 200 $mg.L^{-1}$, beyond which a progressive attenuation was observed.

Beyond 200 mg.L^{-1}, the concentration effect was totally suppressed and the amount of adsorbed dyes became constant at its maximum level, respectively of 72-74 (Telon-red) and ca. 56-57 mg/g (Telon-blue). These values correspond to ca. 0.144 and 0.09 mmol.g^{-1}, respectively, and are almost in the same magnitude as those of figure 4.

This reveals an appreciable affinity of NaMt towards Telon-dyes. According to some results[37-39], adsorption of Telon dyes on NaMt involves ion-exchange and reduction of the dye mobility when "bridged". Nonetheless, one still strongly believes that the contribution of cation exchange sites to dye adsorption, if any, might not be significant, because the maximum amounts of adsorbed dye($\boldsymbol{Q_{max}}$) still remained much lower than the CEC value of NaMt (0.95 meq.g^{-1}).

This adsorption enhancement was often explained in terms of bridging process between the ≡(Metal-O-Si)-H or ≡(Si-O-Si) sites of the surface of NaMt and Telon dyes through the divalent Cu(II) cations[40,41]. This may involve the formation either of ≡(Metal-O-Si)-Cu-Dye via proton release or of ≡(Si-O-Si)---Cu-Dye bridges via pure electrostatic interactions, as for metal cation-chitosan-montmorillonite systems[1,30,31]. On organo-Mt, the relatively lower amount of adsorbed Telon-blue should arise mainly from its lower organophilic character, due to the presence of two exchangeable groups, as compared to Telon-red.

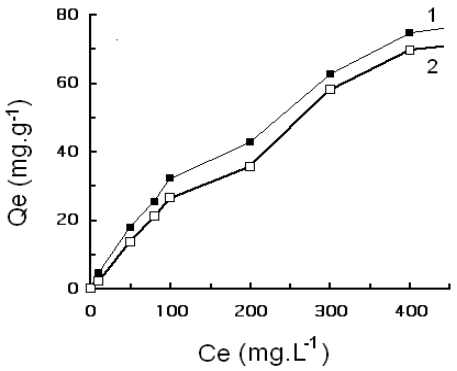

Figure 11. Adsorption isotherm for Telon-red.
1**.** Organo-Mt; 2**.** NaMt.
T = 21°C; t = 90 min; [Cu(II)] = 0.01 M

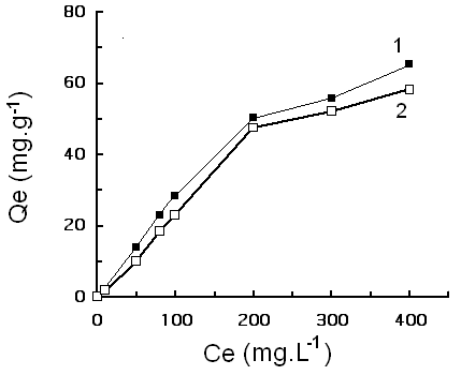

Figure12. Adsorption isotherm for Telon-blue.
1.Organo-Mt; 2**.** NaMt.
2. T = 21°C; t = 90 min; [Cu(II)] = 0.01 M

As compared to the starting NaMt material, improved adsorption capacities were obtained on p-TphPMB-Mt (Figures 11 and 12). The maximum amount of adsorbed dye ($\boldsymbol{Q_{max}}$) was of 76-77 mg.g^{-1}for Telon-red and of 65-66 mg.g^{-1}for Telon-blue. This slight enhancement of the adsorption capacity was attributed to the effect of the clay mineral intercalation by the p-diphosphonium cation, in agreement with previous work[42]. Insertion of organic species within the interlay space is expected to induce an increase in the organophilic character of montmorillonite. This is supposed to induce an enhancement of hydrophobic interactions of the organic dye with diphosphonium ions and the remaining non-covered portion of siloxane surface[43].

Dye adsorption modeling on p-organo-Mt

Similar isotherm investigations were also achieved on p-TphPMB-Mt adsorbent resulting from NaMt intercalation with p-diphosphonium cations. In a first attempt by applying Langmuir's model, only moderate linearity was noticed for Telon-red adsorption (Figure 13).

Adsorption of Telon-blue did not seem to correlate with Langmuir's model. This specific behavior of Telon-blue must be due to its bulkier molecule. In contrast, Freundlich's model

turned out to be more adequate. Indeed, better linearity was observed for Telon-red within the whole range of concentration investigated, and to a lesser extent for Telon-blue (Figure 14).

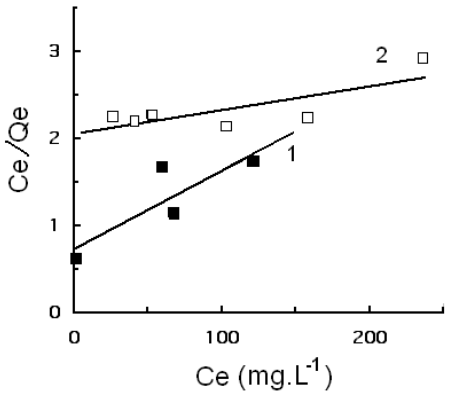

Figure 13. Langmuir adsorption isotherms on p-diphosphonium-Mt.
1**.** Telon-red; 2**.** Telon-blue.
T = 21°C; t = 90 min; [Cu(II)] = 0.01 M

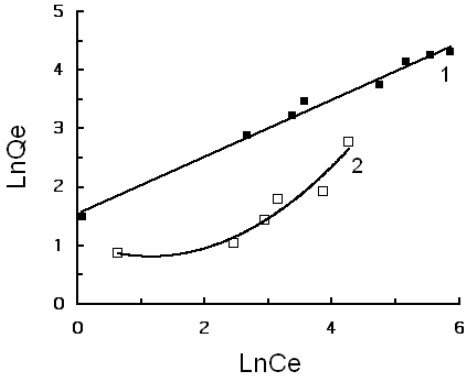

Figure14. Freudlich adsorption isotherms on p-diphosphonium-Mt.
1. Telon-red: n = 0.723; 2. Telon-blue: n = 0.489.
T = 21°C; t = 90 min; [Cu(II)] = 0.01 M

For the latter, Freundlich's model was valid only within a narrower range, more specifically towards medium to high ***Ln(Ce)*** values. These results demonstrated once again that the chemical structure and size of Telon-blue molecules played a significant role, which remains to be thoroughly elucidated through deeper insights. This is why investigations have to be pursued in this direction.

Conclusion

The presence of Cu (II) ions turned out to improve significantly the adsorption of Telon-red and Telon-blue dyes on Na-montmorillonite, presumably thanks to the previous formation of a Cu(II) exchanged Telon-dye form. The two Telon-dyes adsorbed differently, and the dye molecular configuration might play a key-role in the adsorption process. In all cases, the amount of Telon-red removed was higher than that of Telon-blue.

Na-montmorillonite intercalation with p-diphosphonium salts showed improved affinity towards Telon-dyes in the presence of Cu(II) cations in aqueous media.

The Cu(II)-dye adsorption on NaMt better obeyed second pseudo-order kinetics, while the adsorption isotherms correlated with Freundlich’s model. Adsorption on p-organo-Mt also obeyed Freundlich's model within the entire concentration range for Telon-red, but only at high concentrations for Telon-blue.

Acknowledgements

We gratefully acknowledge The CMEP-TASSILI N° 10 MDU799 for their financial support.

Experimental Section

Organo-montmorillonite preparation

The same montmorillonite-rich material as that obtained by bentonite purification in a previous work[10] was used in the present investigations. This material contained mainly montmorillonite (85 %), quartz (10 %) and cristoballite (4 %), and had a cation exchange capacity (CEC) of 95 meq for 100 g of NaMt. Before and after intercalation, the Na-form samples (NaMt)[44,45] were fully characterized through X-ray fluorescence spectroscopy (PHILIPS PW 3710) and X-ray diffraction (Philips X-Pert diffractometer, Ni filtered Cu Kα radiation, λ = 1.5406 Å). The specific surface area was estimated via BET analyses (Nova-1000 instrument, N_2) according to a procedure fully described elsewhere[10]. Further, intercalation of NaMt with para-bis(triphenyl phosphonium methylene)-benzene-dichloride (TphPMB) gave rise to p-diphosphonium organo-montmorillonite (p-TphPMB-Mt), as previously reported[46].

Adsorption kinetics and isotherms

Aqueous solutions containing 100 mg/L of Telon-red ($C_{22}H_{16}N_3NaO_6S_2$, M = 505.5 g. mol^{-1}) and Telon-blue ($C_{22}H_{14}N_6Na_2O_9S_2$, M = 616.49 g.$mol^{-1}$) dyes with intrinsic pH values of 6.7 and 5.1 were used. These organic dyes absorbed at λ_{max} = 500.4 and 608.9 nm respectively (Perkin-Elmer-Lambda 800 UV–Vis spectrophotometer). Between 750-900 nm Telon-red and Telon-blue do not absorb. In the present investigations, the so-called meta-mordanting technique was used[21,22].

Dye adsorption kinetics was performed at 21°C. Amounts of 0.02 g of dry NaMt or organo-Mt were mixed with 10 mL of 100 mg.L^{-1}dye solution under stirring for 5 min in the presence of a constant Cu(II) ions concentration (0.01 M). The mixtures at their intrinsic pH were then stirred at room temperature for 180 min. Periodical sampling was carried out and the dye concentration was periodically measured through UV visible. The amount of dye adsorbed was the difference between the initial amount measured than in solution after adsorption. Besides, adsorption isotherms were obtained at 21, 36, 46 and 56 °C by contacting 0.02 g of dry NaMt or p-organo-Mt with 10 mL of dye solution at various concentrations (10 - 500 mg/L) under continuous and vigorous stirring.

For both kinetics and isotherm study, samples of the supernatant were centrifuged, and UV-Vis spectrophotometry measurements were performed. The specific wavelengths of Telon-blue and Telon-red did not change in time, and provided accurate measurements of the optical density and precise assessments of the amount (mg) of dye adsorbed per gram of adsorbent (Qt). The maximum adsorption capacity (Q_{max}) was defined as being the highest Qt value obtained after reaching equilibrium.

The amount of dye or copper fixed per gram of adsorbent was determined by the following relation (6):

$$Q_t = (C_0 - C_t).V / m \qquad (6)$$

where C_0 and C_t denote the initial and at time t concentrations of dye in the aqueous phase (mg/g), V is the volume of the aqueous phase (L), m is the weight of adsorbent used (g).

References

1 - E. Assaad, A. Azzouz, D. Nistor, A. V. Ursu, T. Sajin, D. Miron, F. Monette, P. Niquette, R. Hausler, Appl. Clay Sci., **2007**, *37*, 258–274.
2 - J. Y. Bottero, K. Kathib, Water Res., **1994**, *28*, 483-490.
3 - S. A. Boyd, Environ. Sci. Technol., **1996**, *9*, 24-28.
4 - S. A. Boyd, G. Sheng, B. J. Trappen, Environ. Sci. Technol., **2001**, *35*, 4227-4234.
5 - D. C. Rodriguez- Sarmiento, J. A. Pinzon-Bello, Appl. Clay Sci., **2001**, *18*, 173-181.
6 - M. K. Sang, J. B. Dixon, Appl. Clay Sci., **2001**, *18*, 111-112.
7 - M. A. N. Lawrence, R. K. Kukkadpu, S. A. Boyd, Appl. Clay Sci., **1998**, *13*, 13-20.
8 - M. A. Didi, B. Makhoukhi, A. Azzouz, D. Villemin, Appl. Clay Sci., **2009**, *42*, 336-344.
9 - B. Makhoukhi, M. A. Didi, D. Villemin, A. Azzouz, Grasas Aceites, **2009**, *60*, 343-349.
10 - B. Makhoukhi, M. A. Didi, H., Moulessehoul, A. Azzouz, D. Villemin, Appl. Clay Sci., **2010**, *50*, 354-361.
11 - N. Al-Bastaki, F. Banat, Resour. Conserv. Recycling, **2004**, *41*, 103-114.
12 - S. A. Boyd, W. F. Jaynes, Appl. Clay Sci., **1993**, *1-4*, 17-30.
13 - A. S. Ozcan, B. Erdem, J. Hazard. Mater., **2005**, *135*, 141-148.
14 - A. S. Ozcan, J. Hazard. Mater., **2006**, *142*, 165-174.
15 - Y. H. Shen, Chemosphere, **2001**, *44*, 989–995.
16 - G. Sheng, S. Xu, S. A. Boyd, Water Res., **1996**, *30*, 1483–1489.
17 - M. Wieczorek, A. Krysztafkiewicz, T. Jesionowski, J. Phys. Chem. Solids, **2004**, *65*, 447–452.
18 - M. Arroyo, M. Suarez, M. Lopez-Manchado, J. Fernandez, J. Nanosci. Nanotechnol., **2006**, *6*, 2151–2154.
19 - A. Hartwig, D. Putz, M. Schartel, M. Wendschuh-Josties, Macromol. Chem. Phys., **2003**, *204*, 2247–2257.
20 - W. Xie, R. Xie, W. Pan, D. Hunter, B. Koene, Chem. Mater., **2002**, *14*, 4837–4845.
21 -International Union of Pure and Applied Chemistry (IUPAC), **1997**. Compendium of Chemical Terminology, 2nd ed. Compiled by A. D. McNaught and A. Wilkinson. Blackwell Scientific Publications, Oxford, **1997**.
22 - R. D. Lillie, P. Pizzolato, P. T. Donaldson, Histochemistry. **1976**, *49*, 23-35.
23 -T. Bechtold, R. Mussak, Handbook of Natural Colorants. John Wiley and Son, Chichester (UK), **2009**, pp.337.
24 - B. Tabak, S. F. Afsin, H. Icbudak, J. Therm. Anal. Calorim., **2005**, *81*, 311–314.
25 - J. Y. Yoo, J. Choi, T. Leer, J.W. Park, Water Air Soil Poll., **2003**, *154*, 225-237.
26 - M. Crocker, R. M. Herold, J. Mol. Catal., **1991**, *70*, 209-216.
27 - R. Margalef, P. Salagre, E. Fernandez, C. Claver, Catal. Lett., **1999**, *60*, 121–123.
28 - J. W. Park, P. Jaffe, Environ. Sci. Technol., **1993**, *27*, 2559–2565.
29 - R. Gullick, W. Weber, Environ. Sci. Technol., **2001**, *35*, 1523–1530.
30 - B. Makhoukhi, M. A. Didi, D. Villemin, Mater. Lett., **2008**, *62*, 2493–2496.
31 -A. Azzouz, Interactions Chitosane – particules colloidales: Synergie avec les argiles. Chapter 12. In:Crini, G., Badot, P. M., Guibal, E. (Eds). Chitine et Chitosane – Du biopolymère à l'application: Presses Universitaire de Franche-Comté, Université de Franche-Comté, Besançon, France, **2009**, pp. 231-255.
32 - A. Azzouz, Chitosan and derivatives– behavior in dispersed state and applications. In: Davis, S. P. (Ed). Chitosan: Manufacture, Properties, and Usage. Series: Biotechnology in Agriculture, Industry and Medicine, Publisher: Nova-Publishers, New-York, USA, **2010**, 4th quarter.
https://www.novapublishers.com/catalog/product_info.php?products_id=12712.
33 - Y. S. Ho, D. A. J. Wase, C. F. Forster, Environ. Technol., **1996**, *17*, 71-77.
34 - A. S. Özcan, A. Özcan, J. Colloid Interf. Sci., **2004**, *276*, 39–46.

35 - A. K. Bajpai, L. Rai, Indian J. Chem. Techn., **2010**, *17*, 17-27.
36 - N. Kannan, M. M. Sundaram, Dyes Pigments, **2001**, *51*, 25-40.
37 - W. J. Weber, J. C. Morris, J. Sanitary Eng. Div. Am. Soc. Civil Eng., **1963**, *89*, 31–39.
38 - A. Mastalir, Z. Kiraly, G. Szollosi, M. Bartoky, J. Catal., **2000**, *194*, 146–152.
39 - H. A. Patel, R. S. Somani, H. C. Bajaj, R.V. Jasra, Curr. Sci. India, **2007**, *92*, 1004–1009.
40 - J. Baham, G. Sposito, J. Environ. Qua., **1994**, *23*, 147–153.
41 -G. Grigoropoulou, P. Stathi, M. A. Karakassides, M. Louloudi, Y. Eligiannakis, Colloid Surface A, **2008**, *320*, 25-35.
42 - S. J. Anderson, G. Sposito, Soil Sci. Soc. Am. J., **1991**, *55*,1569–1576.
43 -R. A. Schoonheydt, C. T. Johnston, Surface and Interface Chemistry of Clay Minerals, in: Bergaya, F., Lagaly, B. K. J., G. (Eds), Handbook of Clay Science – I. Developments in Clay Science. Elsevier, Amsterdam, **2006**, pp. 87-113.
44 - M. B. McBride, Environmental Chemistry of Soils, Second Ed., Oxford University Press, **1994**, pp. 352.
45 -A. Azzouz, D. Messad, D. Nistor, C. Catrinescu, A. Zvolinschi, S. Asaftei, Appl. Catal. A-Gen., **2003**, *241*, 1-13.
46 -A. Azzouz, D. Nistor, D. Miron, A. V. Ursu, T. Sajin, F. Monette, P. Niquette, R. Hausler, Thermochim. Acta, **2006**, *449*, 27-34.